Naval Research Laboratory
Washington, DC 20375-5320

NRL/MR/8123--97-8112

Laser Diode Assembly Testing and Characterization

PETER B. ROLSMA
G. CHARMAINE GILBREATH
AMEY R. PELTZER
JOSHUA H. RESNICK
MICHAEL R. CORSON
CHRISTOPHER J. ROLLINS

Advanced Systems Technology Branch
Space Systems Development Department

November 28, 1997

REPORT DOCUMENTATION PAGE

Form Approved
OMB No. 0704-0188

1. AGENCY USE ONLY (*Leave Blank*)	2. REPORT DATE	3. REPORT TYPE AND DATES COVERED
	November 28, 1997	Final Report

4. TITLE AND SUBTITLE

Laser Diode Assembly Testing and Characterization

5. FUNDING NUMBERS

6. AUTHOR(S)

Peter B. Rolsma, G. Charmaine Gilbreath, Amey R. Peltzer, Joshua H. Resnick,
Michael R. Corson, and Christopher J. Rollins

7. PERFORMING ORGANIZATION NAME(S) AND ADDRESS(ES)

Electro-Optics Technology Section, Code 8123
Naval Research Laboratory
Washington, DC 20375-5320

8. PERFORMING ORGANIZATION REPORT NUMBER

NRL/MR/8123--97-8112

9. SPONSORING/MONITORING AGENCY NAME(S) AND ADDRESS(ES)

SPAWAR
SAP/FMBMB (AFOY)
Washington, DC 20050-6335

10. SPONSORING/MONITORING AGENCY REPORT NUMBER

11. SUPPLEMENTARY NOTES

12a. DISTRIBUTION/AVAILABILITY STATEMENT

Approved for public release; distribution unlimited.

12b. DISTRIBUTION CODE

13. ABSTRACT (*Maximum 200 words*)

An investigation has been conducted to study the response of two Laser Diode Assembly (LDA) components over a range of nominal operating conditions. Each LDA was comprised of a multi-stripe gain guided laser diode array coupled to a length of multi-mode fiber. The components were tested over a temperature-current parameter space. The LDAs were modulated at a rate of 12.5 Mega Bits per Second with a 50% duty cycle. The results of this study could be used as a basis for a mitigation strategy to compensate for Bit Error Rates (BER) compromised by temperature variations and other effects for a spaceborne laser communications link.

14. SUBJECT TERMS

Optical communications
Laser diodes
Laser diode arrays
Free-space optical link

15. NUMBER OF PAGES

30

16. PRICE CODE

17. SECURITY CLASSIFICATION OF REPORT	18. SECURITY CLASSIFICATION OF THIS PAGE	19. SECURITY CLASSIFICATION OF ABSTRACT	20. LIMITATION OF ABSTRACT
UNCLASSIFIED	UNCLASSIFIED	UNCLASSIFIED	UL

NSN 7540-01-280-5500

Standard Form 298 (Rev. 2-89)
Prescribed by ANSI Std 239-18
298-102

TABLE OF CONTENTS

LASER DIODE ASSEMBLY TESTING AND CHARACTERIZATION

I. INTRODUCTION AND MOTIVATION

An investigation has been conducted to study the response of two Laser Diode Assembly (LDA) components over a range of nominal operating conditions. The LDAs were modulated at a rate of 12.5 Mega Bits per Second with a 50% duty cycle. The results of this study could be used as a basis for a mitigation strategy to compensate for Bit Error Rates (BER) compromised by temperature variations and other effects for a spaceborne laser communications link.

The impact of temperature and current on optical pulse amplitude fluctuations and waveforms was investigated for both units. In particular, the effects of varying temperature and current on mode-hopping and waveform structure were quantified by observing the spectral mode patterns and far field time-domain behavior over a range of conditions.

Section II describes laser diode operation and characteristics. Section III describes the spectral mode experiment and the results of those measurements. Section IV describes the far field time-domain measurements. Section V presents the conclusions and recommendations.

II. LDA OPERATION

A. Selection of the Laser Diodes

The architecture of the LDAs selected consisted of a six stripe gain-guided AlGaAs array coupled to a multi-mode optical fiber, 30 cm in length, with a 75 μm core. The two units, designated LDA021 and LDA064, were selected for this investigation because they both met the spectral requirements for a space qualifiable unit and yet have significantly different spectral structures. Also included in this study were laboratory grade laser diodes, including a single stripe, index guided laser and a ten stripe, index guided laser, SDL model 2412. These laser diodes are not representative of flight units, but were included to establish a performance baseline.

B. Operation of Laser Diode Arrays: The P-I Curve

The output of a laser diode is predominantly a function of drive current. For a given temperature and current density, a resonant cavity in the host material is formed such that lasing can be supported. When the drive current reaches the threshold current, the laser diode begins to lase and the light output increases as a function of the drive current. Figure 2-1 shows this Power-Current (P-I) relationship for LDA064 at three operating temperatures. The threshold current

Manuscript approved November 5, 1997

increases as temperature increases, and the slope of the curve above threshold decreases slightly as temperature decreases. These are average operational trends of lasers in general. This study goes beyond these trends and examines fluctuations in laser behavior as a function of changing drive current and operating temperature.

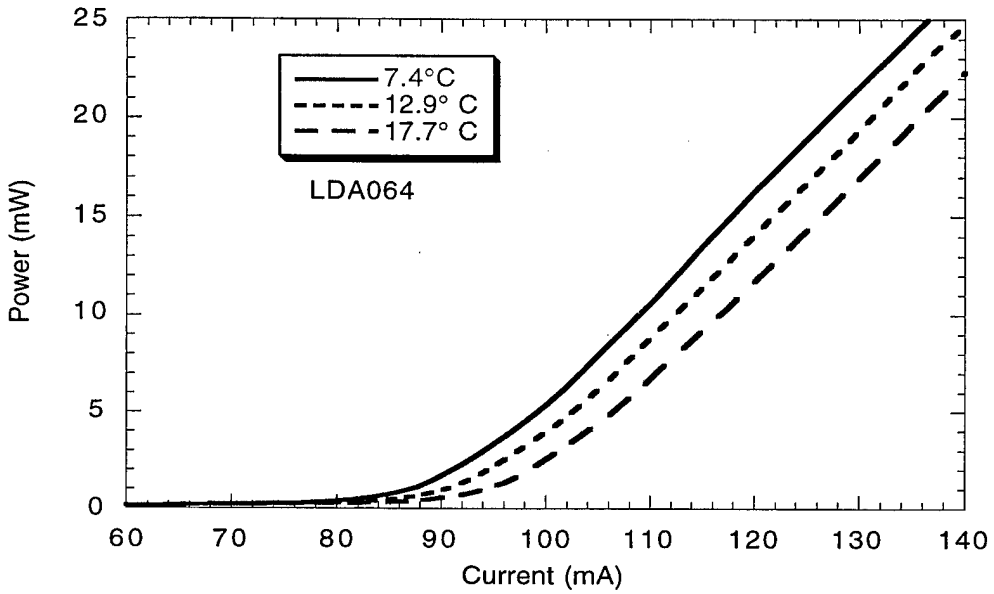

Figure 2-1: P-I Curves for LDA064 at three temperatures

C. Threshold and Temperature Dependence

To quantify the current threshold's dependence on temperature for the units under study, a bench was configured to measure light output vs. drive current of a given laser diode for various temperatures. Software was developed for data acquisition and control and for reducing the data. Threshold dependence on temperature was quantified for four lasers: LDA021, LDA064, the single stripe laser, and the ten stripe laser. The four graphs in Figures 2-2 through 2-5 show the variation in threshold current as a function of operating temperature as a result of this investigation.

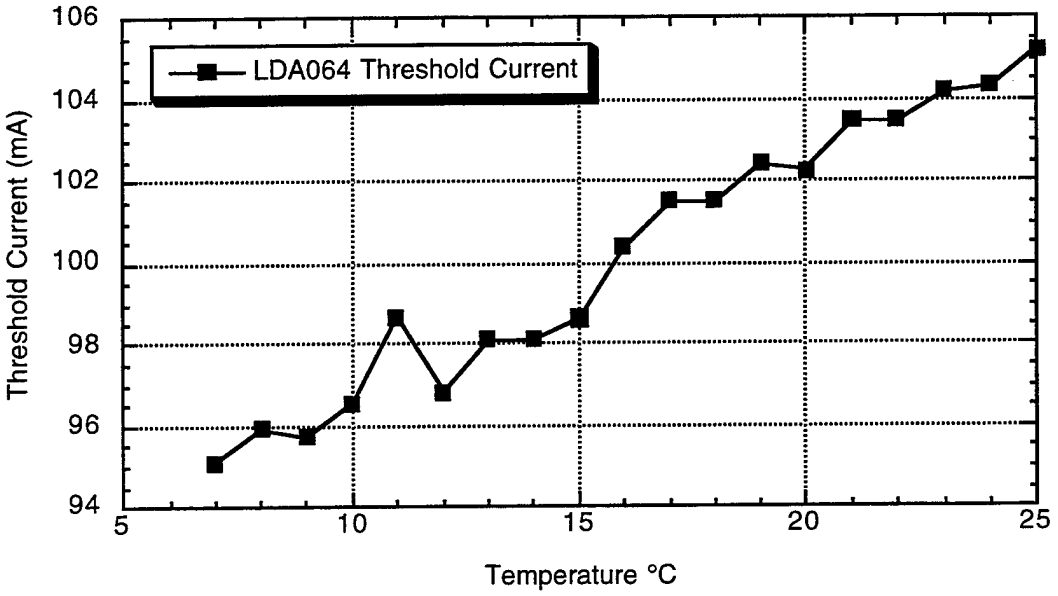

Figure 2-2: Threshold Current vs. Temperature for LDA064.

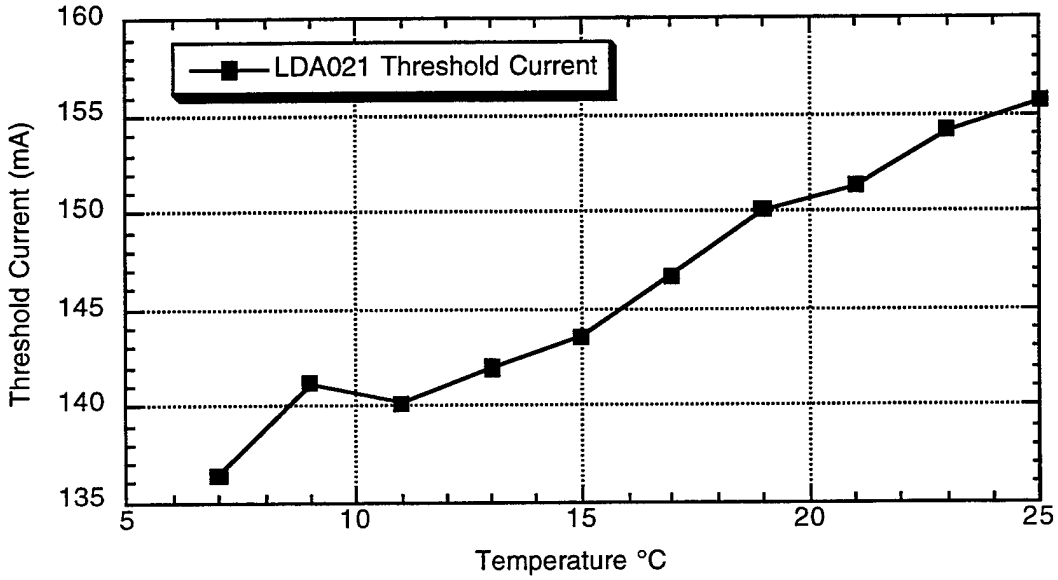

Figure 2-3: Threshold Current vs. Temperature for LDA021.

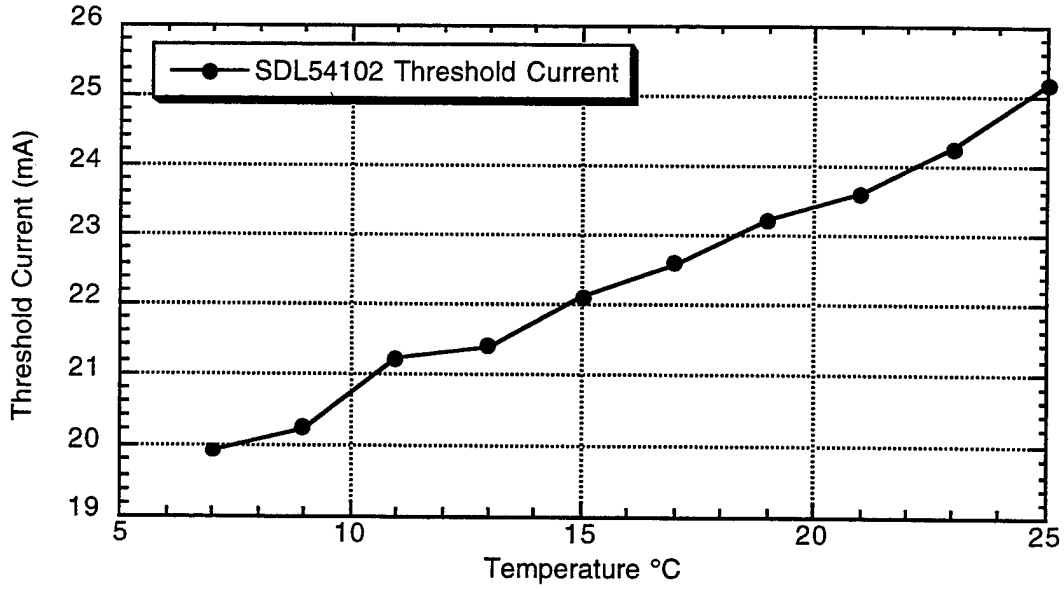

Figure 2-4: Threshold Current vs. Temperature for a Single Stripe Laser.

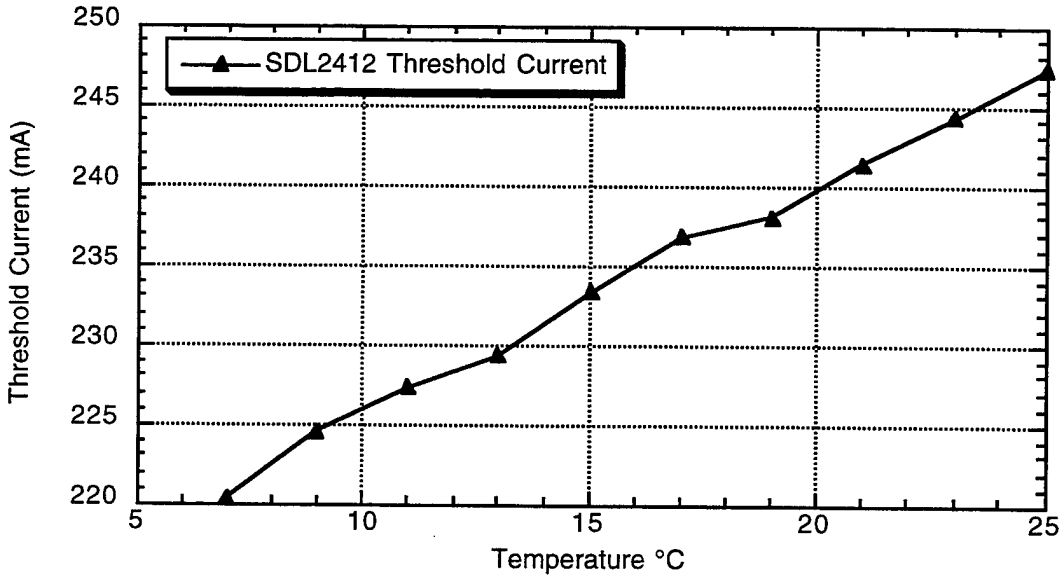

Figure 2-5: Threshold Current vs. Temperature for a Ten Stripe Laser Diode.

By definition, at threshold, the drive current produces sufficient gain to compensate for the cavity loss, and coherent light is emitted. The cavity loss is affected by the precise cavity geometry. To operate the LDAs with constant power output, the drive current must be adjusted to compensate for the shift in threshold due to temperature.

Figures 2-2 and 2-3 show that for the LDAs, there are large deviations from smooth curves. Although, the curves for the single stripe and the ten stripe diodes are smooth when compared to the two LDAs, they still show the need to map the function. The threshold increases with temperature as a general trend, but the small regions where the threshold is decreasing with temperature show the complex nature of the temperature effects for all the lasers. These curves are for DC drive currents, and for the measurements in this study are used to determine the range of operating parameters.

D. The P-I Curve and Definition of Terms

When used in communications, the laser diode drive current is modulated around a DC offset to produce a desired extinction ratio. The extinction ratio is defined as the ratio of the maximum output power, P_{max}, to the minimum power, P_{min}, (see Figure 2-6) and is driven by the maximum and minimum currents, I_{max} and I_{min}, respectively. The extinction ratio for this study was approximately 14:1, with an average power of 7 mW.

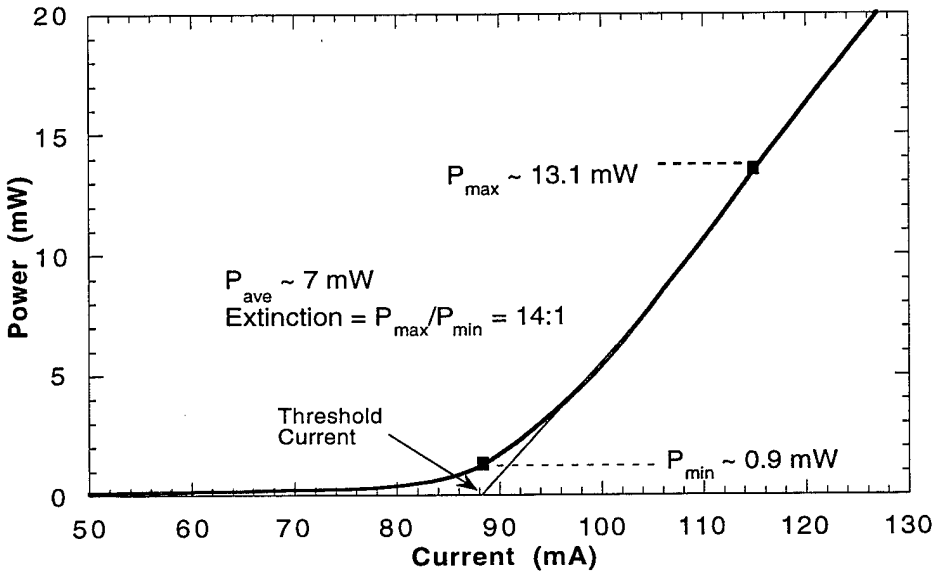

Figure 2-6: The Power-Current Curve of a Laser Diode.

In the experimental testing described in the next two sections, the LDAs were driven using a square wave modulation with a DC bias to replicate a communications link. The DC bias was varied to place I_{min} above and below threshold, as will be discussed at greater length in the report.

E. Spectral Mode Structure

The spectral mode structure of a given laser diode is characterized by the distribution of energy into multiple modes. In a gain-guided architecture, this distribution is a function of current density, temperature and manufacturing defects in the host material. Laser diodes are known to lase in several spectral modes simultaneously, so that light is emitted simultaneously at several closely-spaced wavelengths. The selected LDAs differed significantly in spectral structure. Typical mode patterns for these units can be seen in Figures 2-7 and 2-8. LDA021 shows a broader distribution of energies into multiple modes for a given intensity, while LDA064 shows more of the energy directed into a single mode. For both LDAs, these modes tend to be spaced 0.3 nm apart.

The spectral structure varies with time both on the short time scale associated with typical modulation ($\leq$ 40 ns) and on a longer time scale typical of thermal drift (~ seconds). These energy shifts from one mode to another will cause power versus time deviations. Such shifts cause the output waveform to deviate from a square wave.[1]

[1] W. L. Lippencott, Anne E. Clement, and William C. Collins, "Experimental Measurements of Modal Transients and Theoretical Thermal Modeling of Laser Diodes", Proceedings of the SPIE, Vol. **1219** (1990), pp. 401-416.

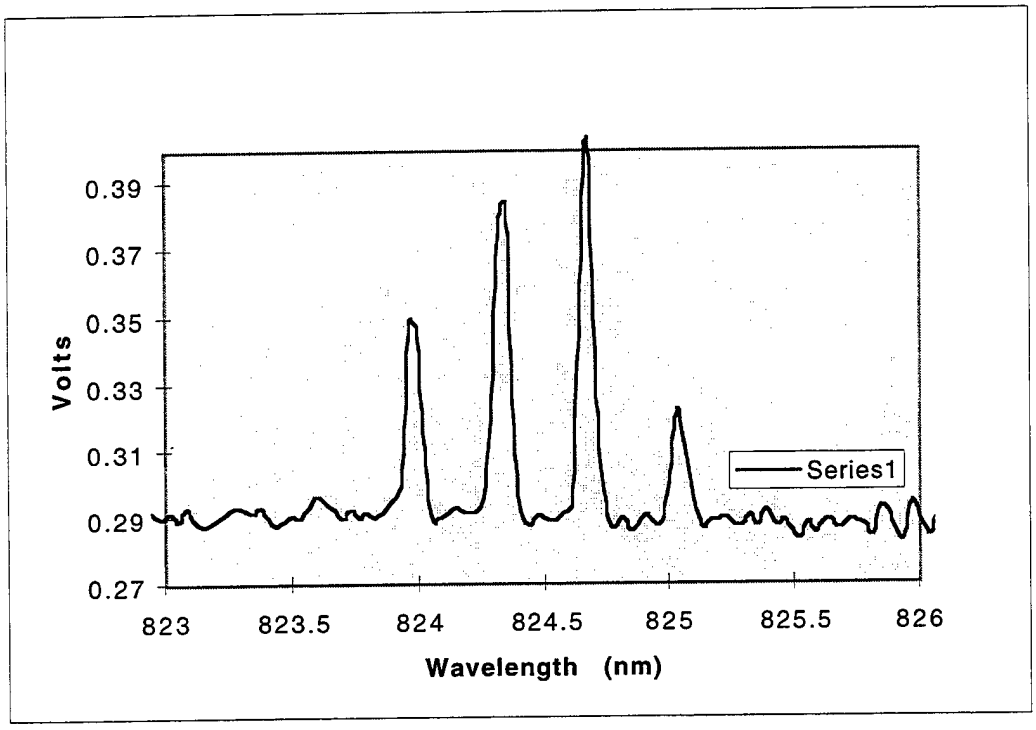

Figure 2-7: Typical Spectral Structure for LDA021.

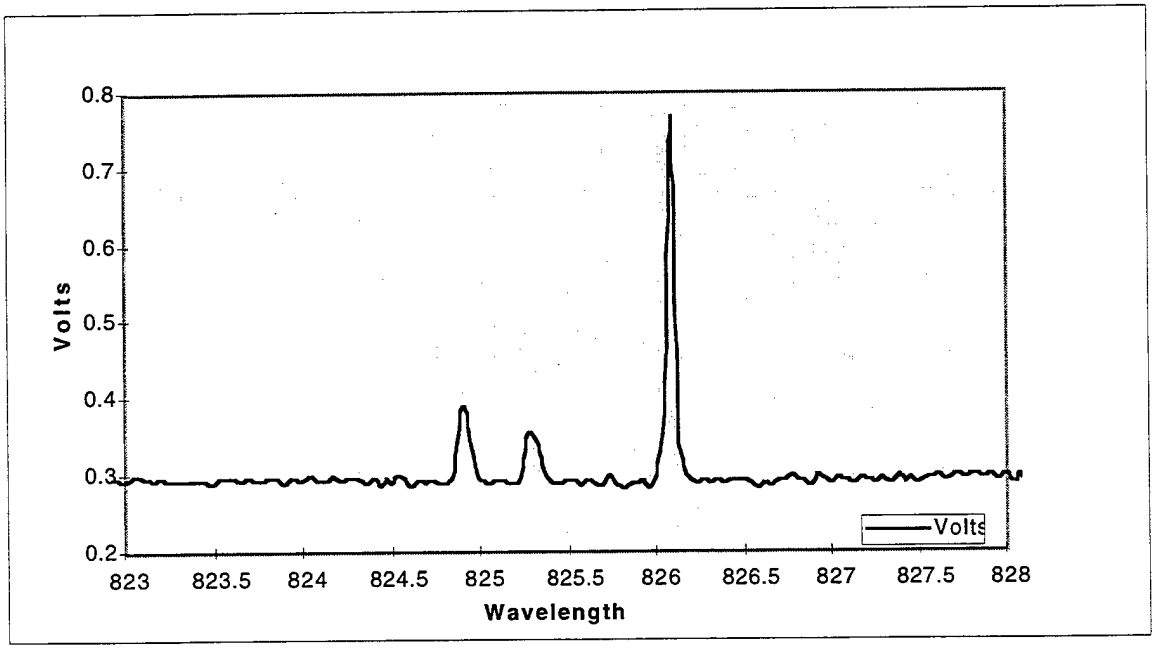

Figure 2-8: Typical Spectral Structure for LDA064

III. Spectral Mode Testing and Analysis

In order to better understand the behavior of the LDAs at different operating conditions, the spectral modes were investigated for different temperatures and drive currents.

A. Experimental Setup

The modal structure measurements required separating the laser output into its spectral mode components. The waveforms of the modes were then recorded under different operating temperatures and drive currents. Figure 3-1 shows the bench configuration used for this investigation.

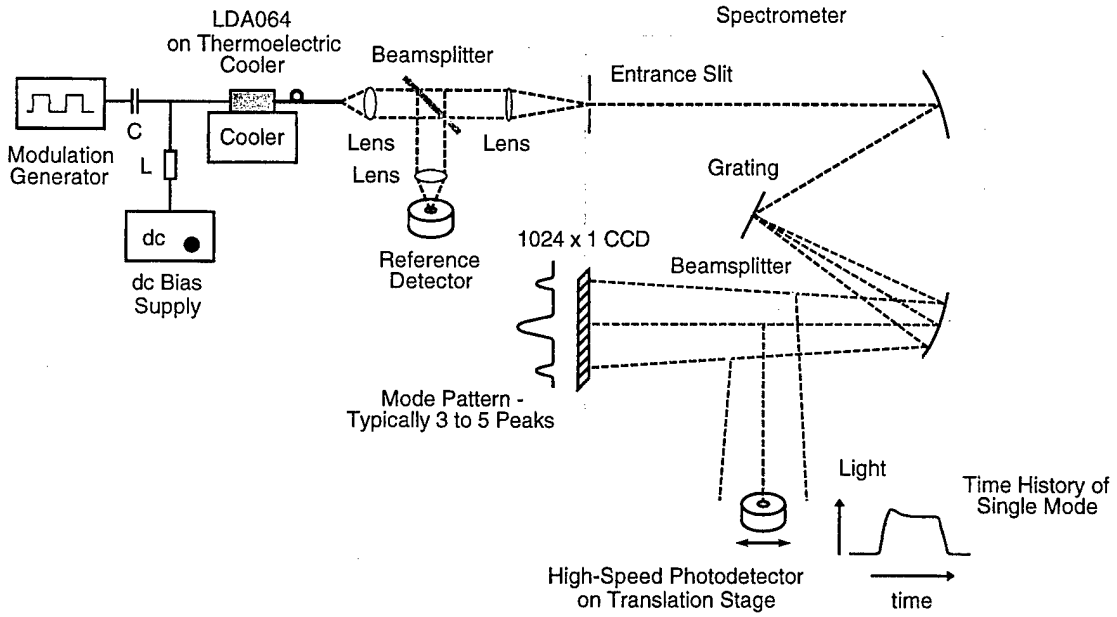

Figure 3-1: Spectral Mode Experimental Bench Configuration.

The laser diode was operated by applying a drive current from a DC current supply. A bias tee added a 12.5 MHz square wave voltage from a waveform generator, resulting in the modulation of the laser with a nominal 12.5 MHz square wave.

The LDA was mounted on a thermoelectric cooler to control the LDA operating temperature. The LDA output was collimated with a lens one focal length from the end of the fiber. The collimated light passed through a beam-splitter where a small fraction of the beam was reflected and focused onto a reference detector in order to monitor the total, spectrally undispersed output. The rest of the beam was focused onto the 25 μm wide entrance slit of a spectrometer. A

second beamsplitter reflected the spectrally dispersed light to a high speed avalanche photodetector (APD), while the remainder of light from the dispersed beam was imaged onto a 1024 x 1 CCD array which enabled observation of the entire mode pattern in real-time.

The spectrometer uses a reference Helium Neon (HeNe) laser which is co-linear with the incident beam. The HeNe laser beam is used to calibrate the wavelength of the incoming beam. The wavelength of each of the modes can be measured to better than 0.05 nm accuracy by the instrument. The APD was mounted on a translation stage, enabling the detector to be moved to monitor each spectral mode individually. The APD has a 300 μm aperture diameter. This size ensured that all light collected was from a specific individual mode; i.e. no light was intercepted from a neighboring mode. The detector also has a sub-nanosecond risetime and therefore is not bandwidth limited, providing enough resolution to accurately measure the modulation waveform of each mode.

The output of the APD was amplified by approximately 80 dB and was directed into a boxcar integrator, where the pulse shape was sampled, averaged over a period of seconds, and recorded.

The individual mode's shape was averaged for a variable period at the integrator. This averaging was necessary due to the limited amount of light transmitted through the spectrometer by a single mode. By observing all the spectral modes' pulse shapes, the energy shift from mode to mode during a modulation pulse could be determined.

B. Experimental Parameters

The LDAs were initially operated from a DC current and voltage modulation level that produced a 7 mW average output and an extinction ratio (high power to low power) of 14 to 1. These initial conditions set P_{min} at 0.88 mW and P_{max} at 13.1 mW. The drive current required for these light levels was different for each temperature. The modulation voltage was kept constant for each laser.

The DC current was then adjusted above and below its initial value while maintaining the square wave modulation voltage. At each current, the averaged pulse shapes of the individual modes were captured and recorded. There were generally two to five spectral modes at each operating condition. These current excursions were repeated for a set of laser diode temperatures over the range of 4° to 14° C at approximately 2° intervals. The resulting matrix of operating conditions contained six bias currents at five operating temperatures for LDA064 and seven bias currents at six operating temperatures for LDA021.

The value of I_{min} with respect to the threshold current was of particular importance. As the bias current was lowered, I_{min} was driven below the laser threshold. As the bias current was increased, I_{min} was driven above threshold. When I_{min} is below threshold, the "turn-on" delay is affected, potentially compromising the symmetry between rise time and fall time for given waveform. For this effort, I_{min} was driven as much as 10 mA below threshold and 8 mA above threshold.

C. Spectral Mode Data Analysis

As described in the last section, the pulse shapes of the individual spectral modes were recorded for a set of operating temperatures and bias currents. The means of quantifying the deviation of the pulse from the ideal response is described in this subsection.

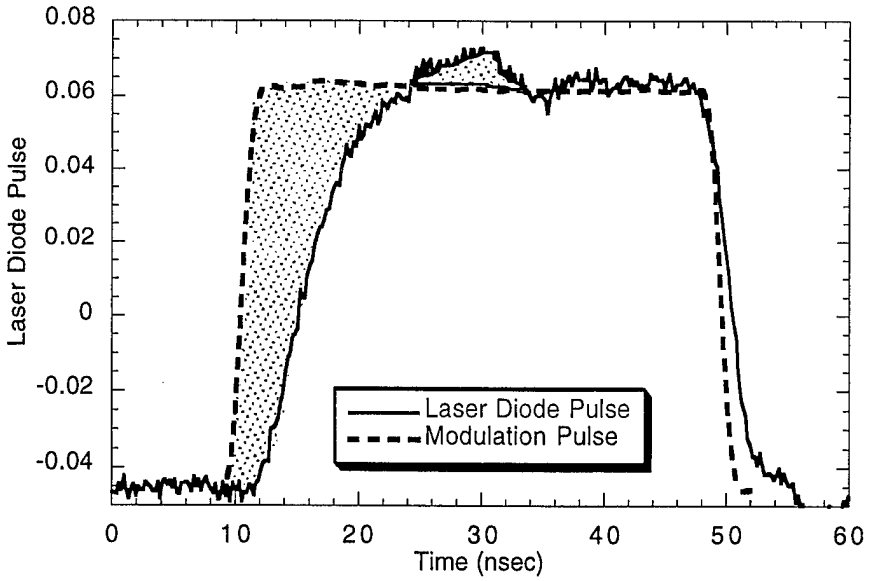

Figure 3-2: Deviation for a Single Mode from LDA021
(Deviant area is shaded.)

Figure 3-2 shows a laser diode pulse overlaid on a normalized drive current pulse. The drive pulse shape was measured at the output of the waveform generator and is not a perfect square wave. This pulse shape was normalized so that its amplitude matched the average amplitude of the laser diode pulse in the latter half of its pulse. The rationale for this normalization is the assumption that transient effects will have dissipated in the latter half. The area by which the light pulse deviated from the normalized drive pulse was then calculated over the first half of the light pulse. This calculated area is the deviant area (see

Figure 3-2). For a single mode, the percent deviation is the ratio of the deviant area to the total area of the pulse, expressed as a percentage. For each operating condition, there are 2 to 5 modes for which the percent deviation was calculated.

The integrated percent deviation for each operating condition is defined as:

Integrated Percent Deviation = Σ Percent deviation of mode • fraction of energy in mode.

The integrated percent deviation for the operating condition is the weighted average of the individual modes' percent deviation. Figure 3-3 shows the percent deviation and fraction of total energy for each mode for LDA064 at a temperature of 12.3° C and a bias current of 99 mA. Using the equation above, the integrated percent deviation was calculated to be 18.9% for these operating conditions.

$$\text{percent deviation} \equiv \sum_{\text{modes}} \text{percent deviation of mode} \bullet \text{fraction of energy in mode}$$

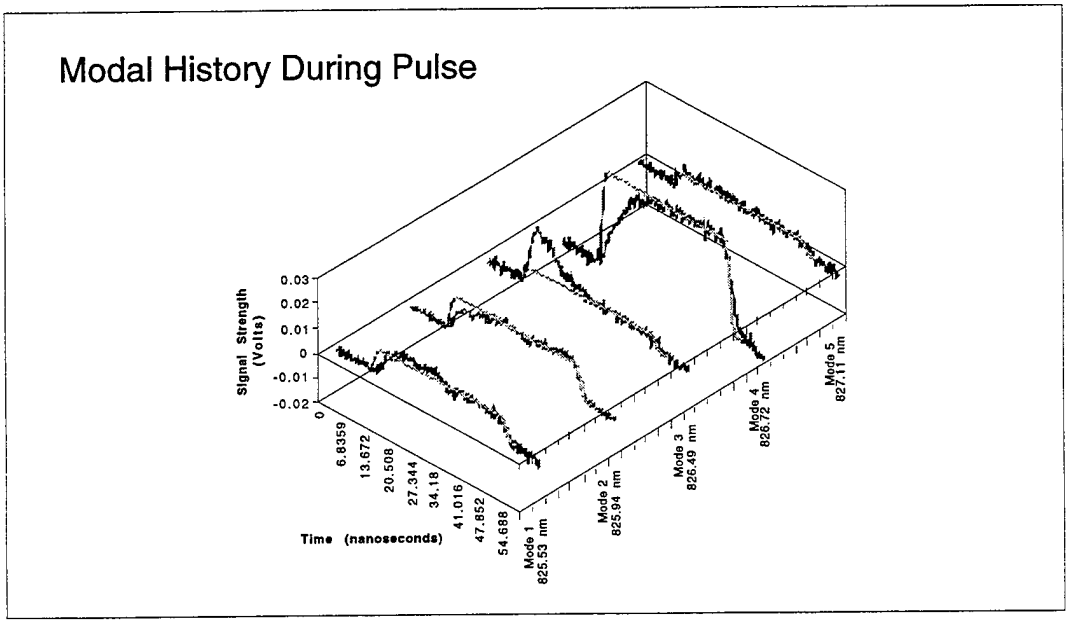

Mode Number	Percent Deviation	Fraction of Energy
1	17%	13%
2	12%	17%
3	42%	14%
4	16%	48%
5	13%	8%

Integrated Percent Deviation =18.9% for LDA064 at 12.3° C, and $I_{min} - I_{threshold} = -1$ mA

Figure 3-3: Example of calculation of percent deviation

D. Results

The measured integrated percent deviation map for LDA064 is shown in Figure 3-4. The current level (I_{min} - $I_{threshold}$) indicates the level above and below threshold. Yellow shaded areas indicate operating conditions for which the deviation is low, while blue indicates operating conditions for which the deviation is high.

I_{min} - $I_{threshold}$ (mA)	6.4° C	8.4° C	10.0 ° C	12.3° C	14.1° C
- 7	19.4%	19.8%	24.6%	15.4%	20.0%
- 6					
- 5					
- 4	13.5%	17.9%	19.9%	15.1%	21.9%
- 3					
- 2					
- 1	17.2%	8.9%	16.2%	18.9%	12.0%
0	- - - -Imin = Threshold Current- - - -				
1					
2	9.0%	8.5%	11.4%	13.2%	8.8%
3					
4					
5	11.5%	9.4%	9.3%	13.2%	6.0%
6					
7					
8	7.5%	7.4%	5.8%	13.1%	12.1%

Figure 3-4: Percent Deviation Map for LDA064

LDA064 shows a fairly clear trend of better performance (less deviation) at the higher currents across all temperatures. As an example, Figures 3-5 and 3-6 show the spectral mode history during the pulse for two operating conditions: 10° C and I_{min} = 7 mA below threshold, and 10° C with I_{min} = 8 mA above threshold. In these figures, the individual mode output pulse shapes are overlaid with a normalized ideal response pulse. The bias current is listed for each graph as is the difference between I_{min} and the threshold current.

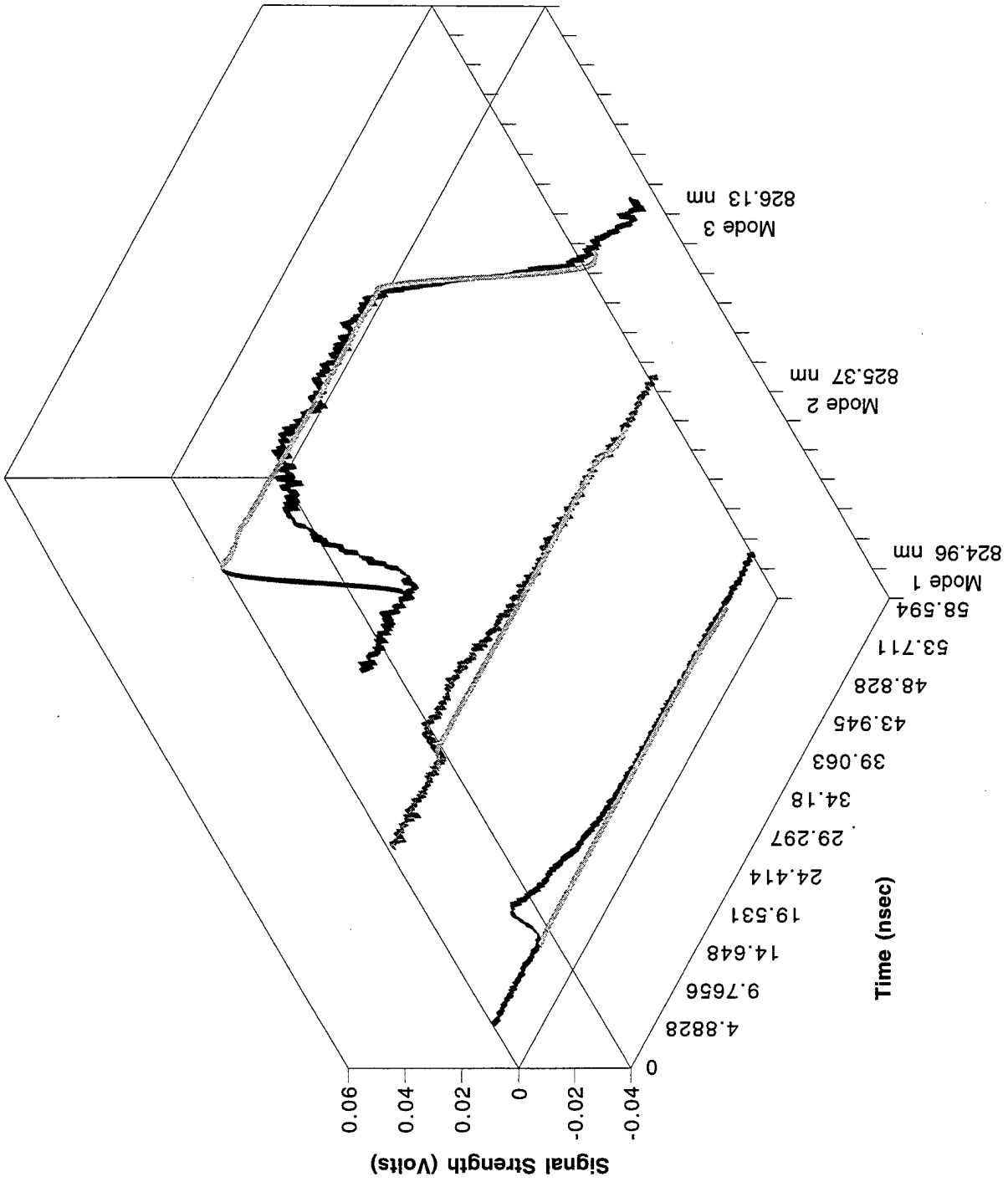

Figure 3-5: Modal History During Pulse SN064, 92 mA (7 mA below threshold current) at 10° C

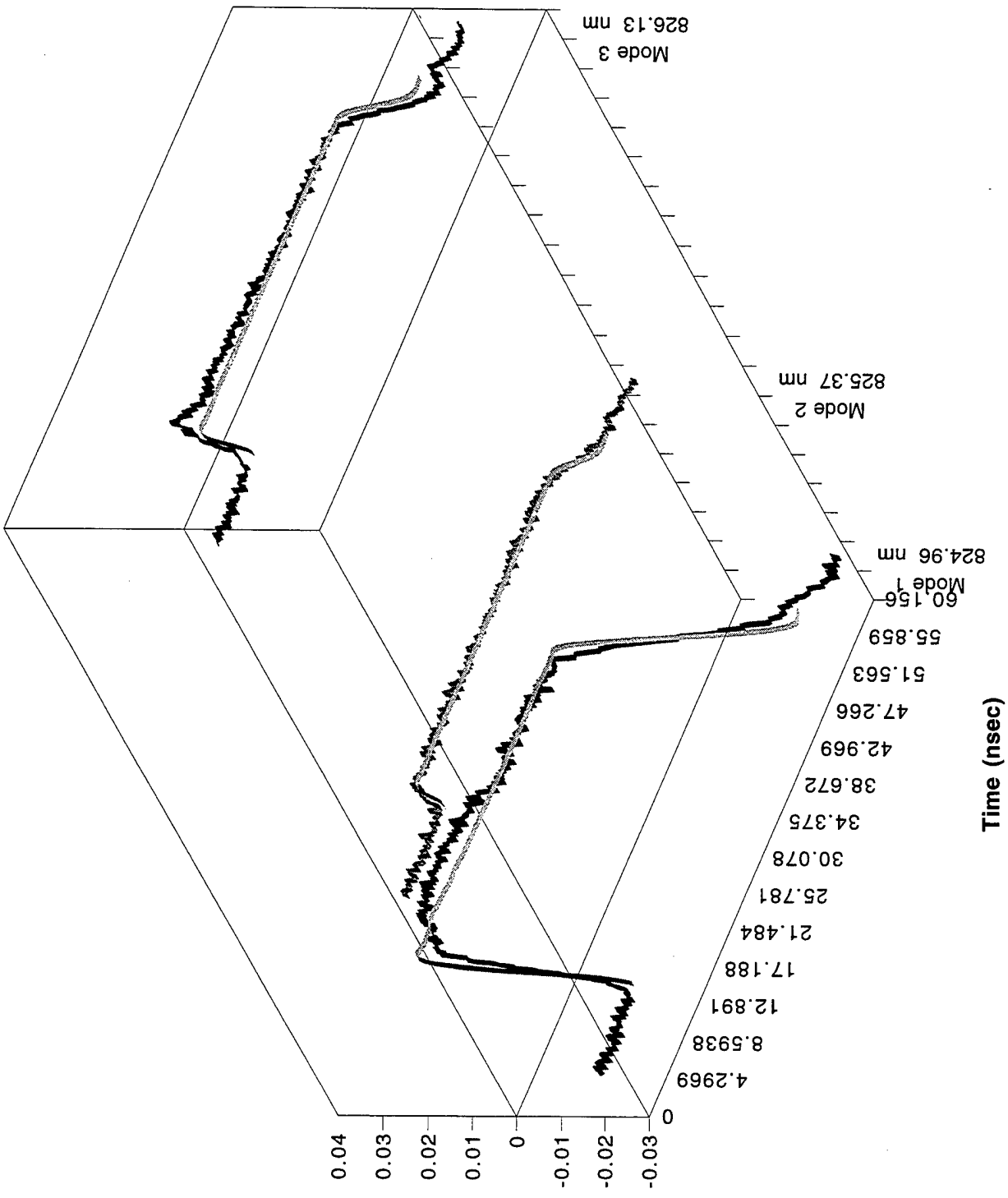

Figure 3-6: Modal History During Pulse SN064, 107 mA (8 mA above Threshold), 10° C

In Figure 3-5 (I_{min} below threshold), it is clear that none of the spectral modes are well-behaved. Modes 1 and 2 rise quickly and then fall to very low light levels during the remainder of the drive pulse, while Mode 3 rises later, maintaining the light level for the duration of the drive pulse. The behavior of the modes shows the energy distribution shifting from Modes 1 and 2, which produce most of the output power at the start of the pulse, to Mode 3 for the latter half of the pulse.

In Figure 3-6 (I_{min} above threshold), all three spectral modes appear well-behaved, matching the normalized ideal response pulse.

The dynamic energy redistribution among spectral modes exhibited in Figure 3-5 might affect the far field pattern. In the far field, this redistribution could appear as a speckle spot increasing in brightness during the pulse, or nearly disappearing during the pulse, depending on whether that portion of the speckle consists mostly of Mode 1 and Mode 2, or mostly of Mode 3. The deviation of the individual spectral modes can cause fluctuation of the speckle pattern on the time scale of individual pulses. Likewise, Figure 3-6 suggests very little transfer of energy between the modes during the pulse, and therefore, a more stable intensity distribution in the far field.

Examining the deviation map in Figure 3-4 again, LDA064 shows a trend of better performance where I_{min} is above the threshold current for all temperatures. However, this trend does not appear in the results from LDA021. Figure 3-7 show the deviation map for LDA021.

I_{min} - $I_{threshold}$	4.2° C	5.6° C	7.5° C	10.1° C	12.3° C	14.5° C
-10	15.6%	17.2%	15.0%	13.8%	11.9%	15.0%
-9						
-8						
-7	14.9%	13.2%	12.9%	17.0%	10.8%	14.0%
-6						
-5						
-4	13.2%	20.6%	12.9%	20.5%	9.2%	9.1%
-3						
-2						
-1	14.2%	18.7%	10.1%	22.4%	15.8%	8.0%
0	----------Imin = Threshold Current ----------					
1						
2	16.9%	18.1%	14.8%	17.1%	18.5%	10.2%
3						
4						
5	17.4%	16.5%	14.5%	15.6%	20.5%	13.7%
6						
7						
8	11.4%	11.1%	11.0%	15.6%	17.3%	8.4%

Figure 3-7: Integrated Deviation Map for LDA021

The trend of improved performance, or reduced deviation, at higher currents independent of temperature which characterized LDA064 is not apparent in LDA021.

LDA021 exhibits no clear trends. For example, at 14.5°C, there is a general trend of better performance at higher currents, while at 12.3°C, there is a general trend of poorer performance at higher currents. Specifically, Figures 3-8 and 3-9 show the modal histories for two operating conditions at 14.5° for LDA021 that show better performance at higher current. Figures 3-8 shows the history at a bias current for which I_{min} is 10 mA below threshold. Mode 1 shows a quick-rising pulse that falls off soon after, while Mode 3 shows a late rising pulse. Figure 3-9 shows the modal history at a bias current for which I_{min} is 8 mA above threshold, and all three modes approximately follow the drive pulse in shape.

At 12.3° C, the opposite trend is apparent. Figure 3-10 shows the modal history for LDA021 at 12.3°, with I_{min} 10 mA below threshold. Unlike the previous graphs showing more deviant behavior below threshold, at 12.3° C, all four modes follow the ideal drive pulse reasonably closely. Figure 3-11 demonstrates the modal history where I_{min} is 5 mA above threshold at 12.3° C, and shows deviant modes.

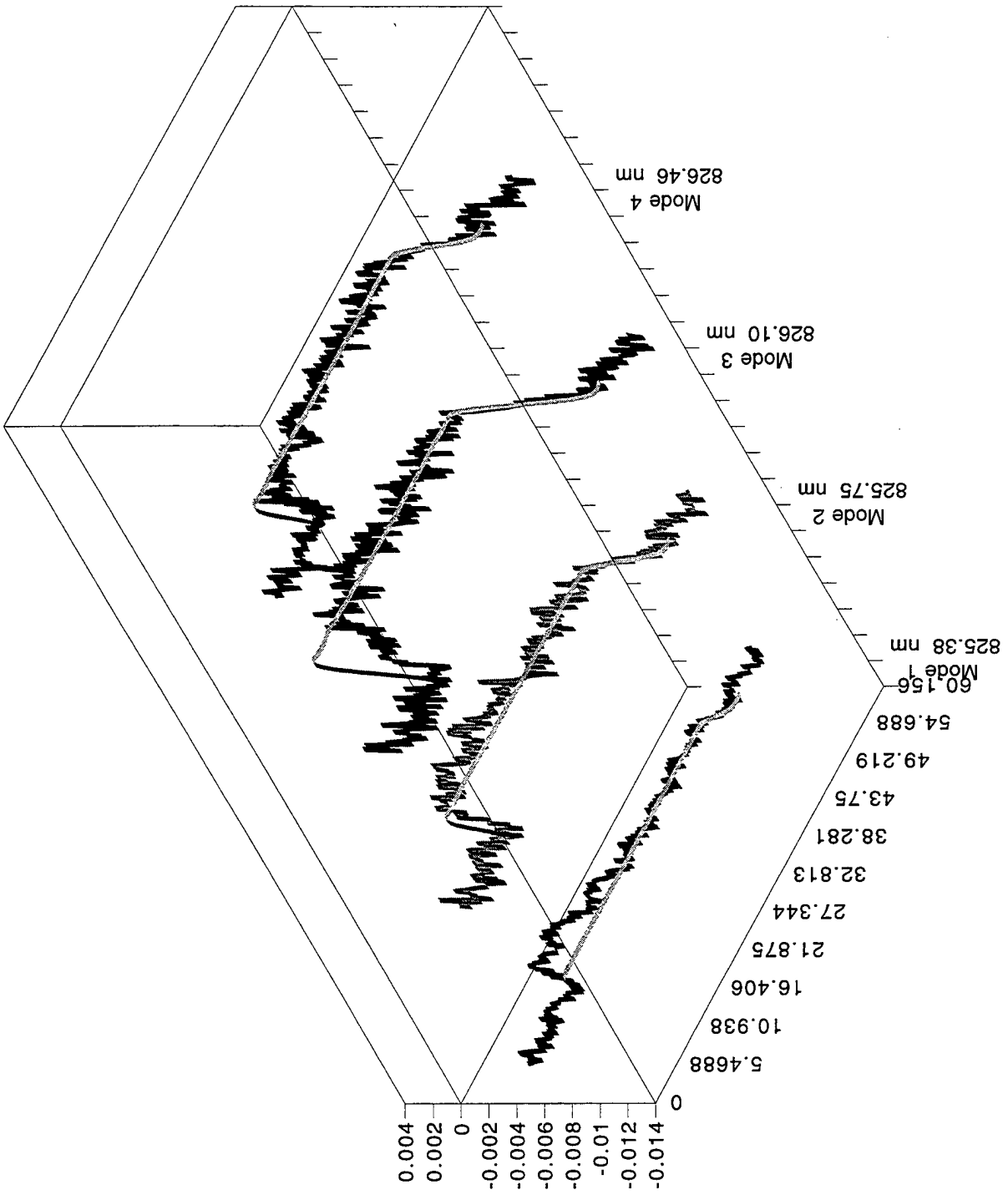

Figure 3-8: Modal History for Pulse SN021, 140 mA (10 mA below threshold) at 14.5° C

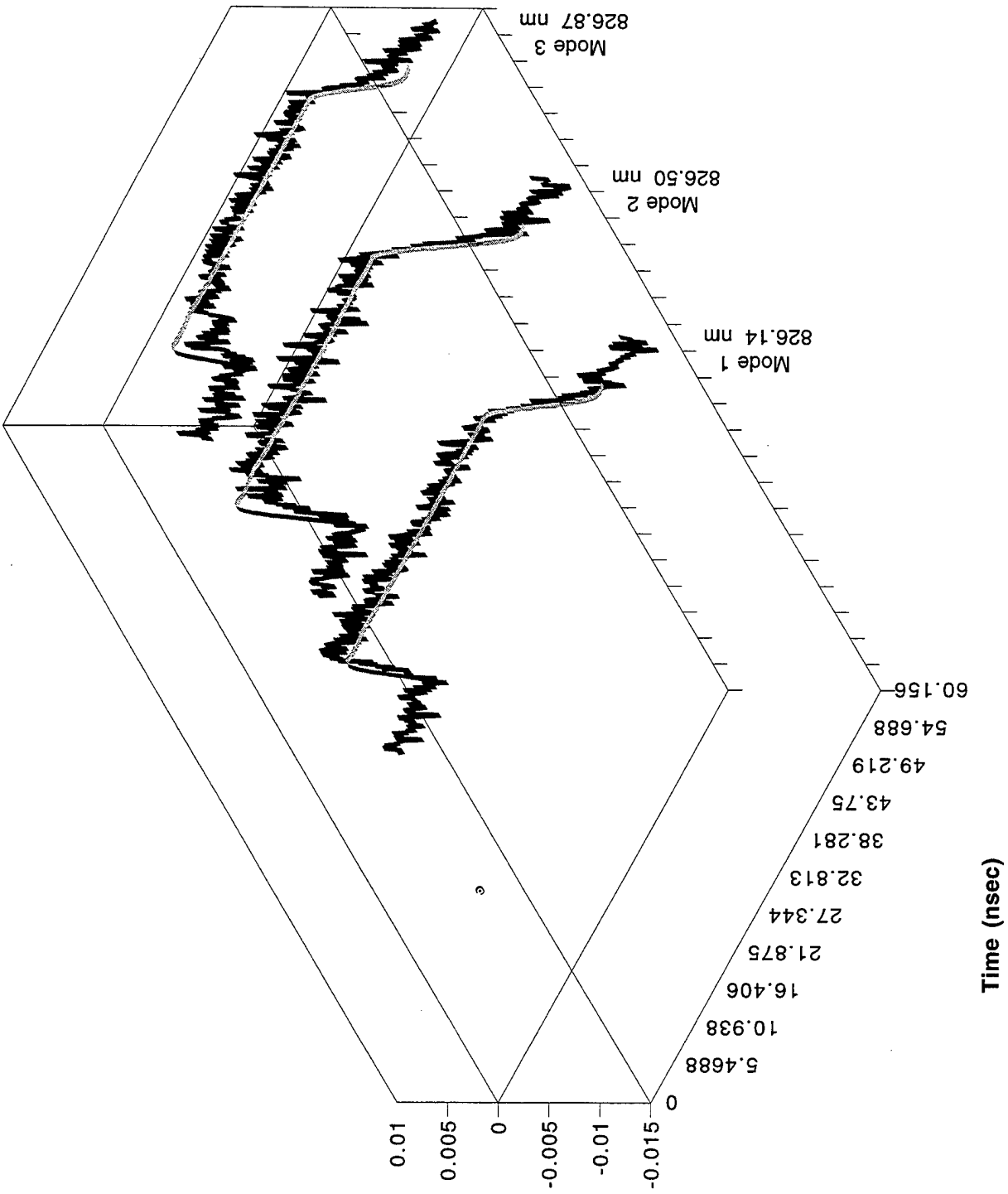

Figure 3-9: Modal History for Pulse SN021, 158 mA (8 mA above threshold), at 14.5° C

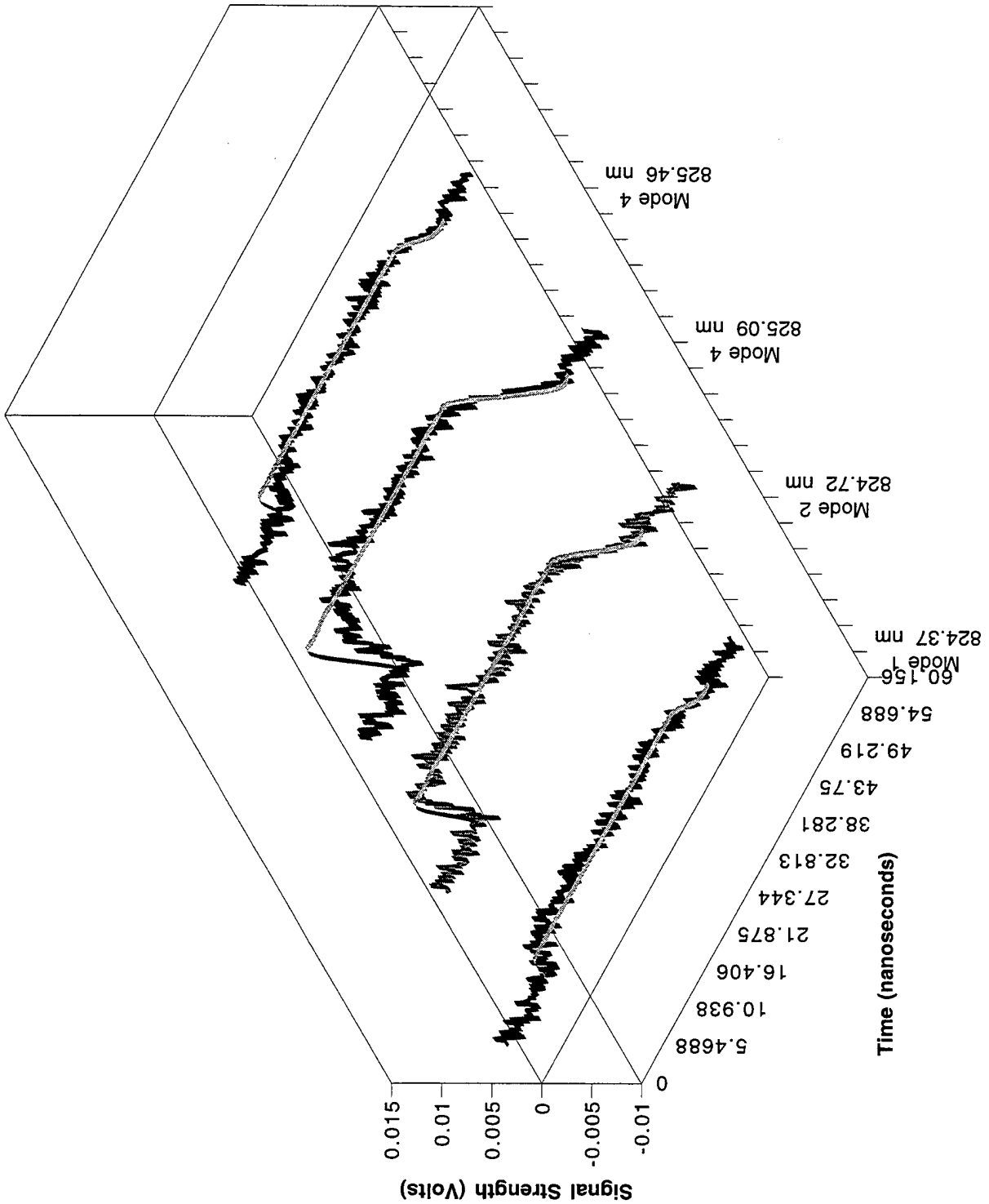

Figure 3-10: Mode History for Modulation Pulse SN021, 137 mA (10 mA below threshold), at 12.3° C

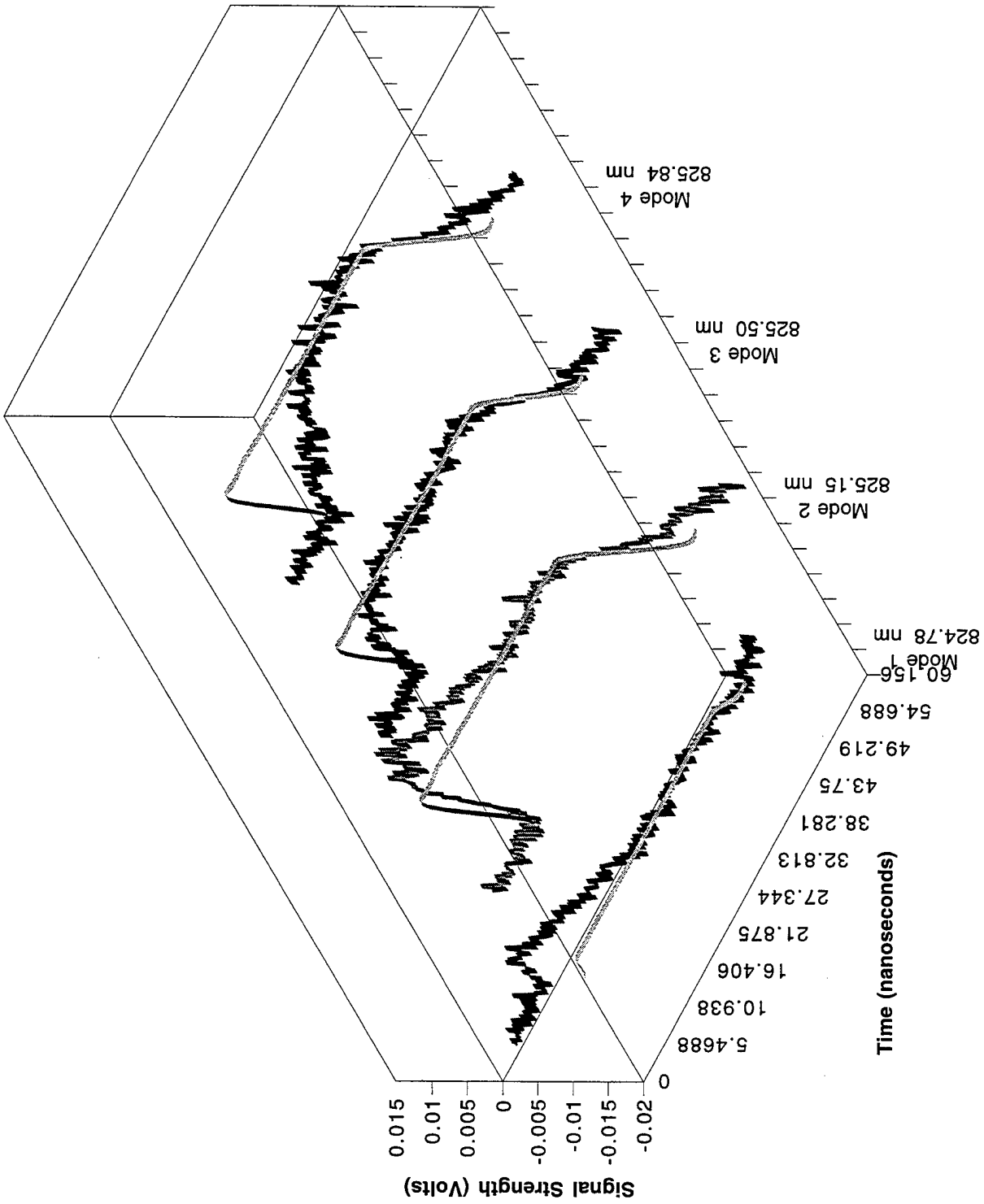

Figure 3-11: Mode History for Modulation Pulse SN021, 152 mA (5 mA above Threshold) at 12.3° C

IV. Far Field Time Domain Waveform Measurements

A. Motivation of Time Domain Measurements

Optical propagation to the far field is a linear operation (**h**(x,y;t)) for the electric field, as shown in Figure 4-1. The measured intensity in the far field is the square of the electric field, and includes interference effects and speckle. Speckle is a function of coherence and describes a condition where the resultant field at any location in space is comprised of the superposition of many contributing wavelets due, in this case, to propagation through different regions of indices of refraction. There are two sources of time dependence of the speckle pattern in this system. The first is slow changes due to geometry. The second is high speed fluctuations due to the time history of laser spectral modes which drive the fiber's spatial modes, and which are of interest in this study. The receiver detects only a small area of the transmitter's propagated beam. Hence, the noise is averaged only over the subtended area and not over the whole beam.

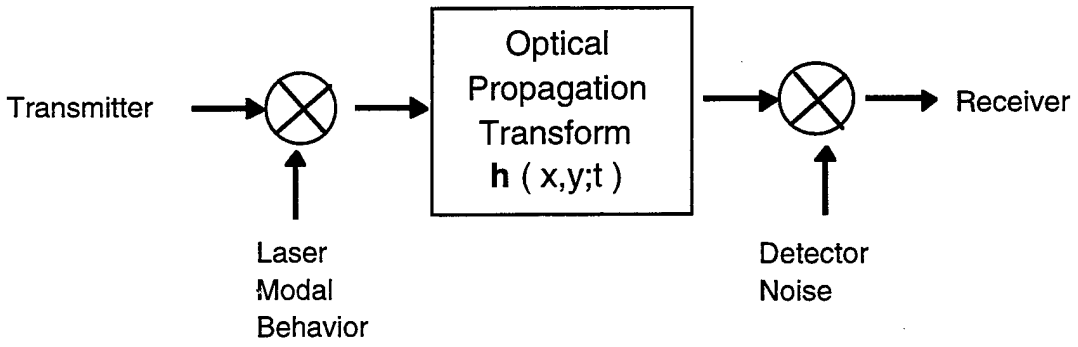

Figure 4-1: Propagation Model

The detected fluctuations can be understood by considering the electric field as a sum of modes. The electric field for each mode propagates linearly, and then the square of the total electric field is detected. The electric field can be decomposed by an expansion in terms of fiber spatial modes. For this fiber with a core diameter of 75 microns and a numerical aperture of 0.3 to 0.33 there are about 4,000 fiber modes per LDA spectral mode. Each of these modes (fiber and LDA) propagates with a linear transform **h** representing the propagation. After propagation, each mode has a new spatial distribution and phase. All of the propagating modes have time-varying phases which interfere with each

other producing intensity fluctuations. This intensity fluctuation was experimentally measured as the temperature and current were varied.

B. Experimental Setup for Time Domain Measurements

To capture waveforms and determine the statistical behavior of the far field laser pulses as a function of temperature and drive current, the configuration shown in Figure 4-2 was used. Experimental propagation with both the speckle size to beam size ratio and receiver aperture to beam size ratio were chosen appropriate for a full scale optical communications link. The distance between the fiber end and the detector was 45 mm. The fiber numerical aperture of 0.3 and the detector area of 0.008 mm^2 for a ratio of detector area to spot area of $1.3x10^{-5}$. The ratio of speckle angular size to beam size was 0.021 for this configuration.

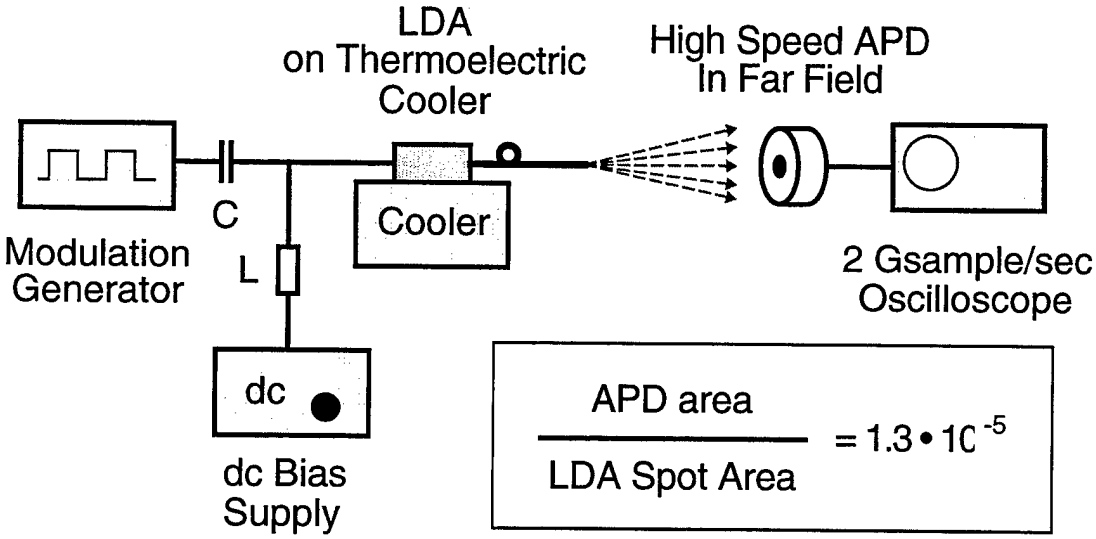

Figure 4-2: Experimental Configuration for Time Domain Waveform Measurements

The detector signal was sampled with a 500 MHz oscilloscope at a 2 Giga-Sample per second rate. The oscilloscope stored 15,000 samples for post-processing and analysis. The post-processing included two steps. The first step was to set the waveform mean to zero. This is equivalent to AC coupling for a representative system. The second step was to set the standard deviation to one. This is equivalent to a system with automatic gain control. The temperature and the DC bias current were varied in the same fashion as in the spectral mode measurements. Figures 4-3 and 4-4 show the effects of changing the current about threshold (99 mA) for LDA064 at 10° C.

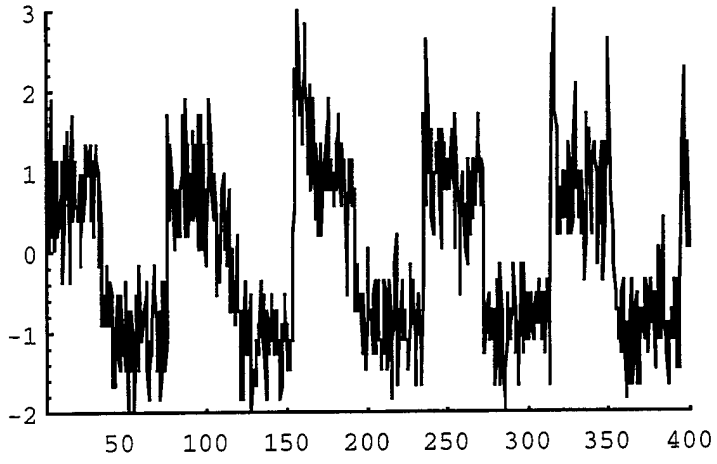

Figure 4-3: Far-Field Modulated Light Intensity for LDA064 at 92 mA (7 mA below threshold), 10° C.

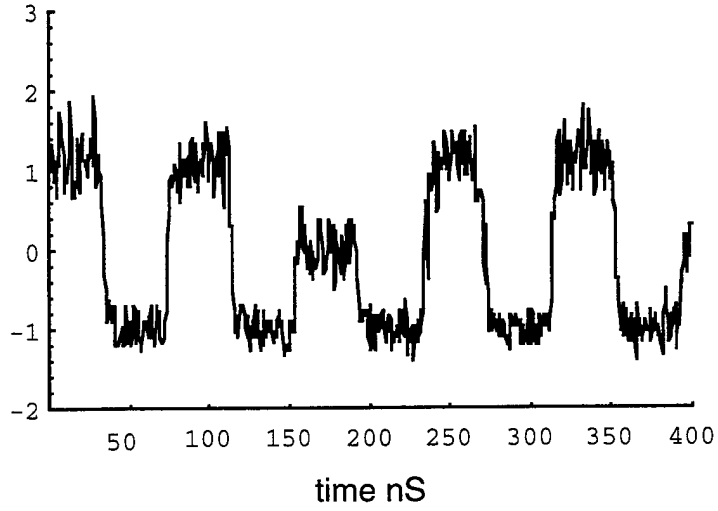

Figure 4-4: Far Field Modulated Light Intensity for LDA064 at 107 mA (8 mA above threshold), 10° C.

Far field time domain measurements were made for both LDA064 and LDA021. In each case the laser was set for an average optical output power of 7 mW and was modulated with a 12.5 MHz square wave. The waveforms shown in Figures 4-3 and 4-4, are five pulses which are comprised of 800 samples. The total data collected for each temperature and current combination was over 93 pulses which corresponds to 15000 samples. To handle this large amount of data, statistical methods were employed. In this experiment, the fluctuations were quantified in terms of a Root Mean Square (RMS) from a perfect square

wave. A typical communication system's BER is a function of the fluctuation about the average signal.

The processing for the RMS figure-of-merit is calculated by the following method: First, the waveform is normalized; then, the absolute value of each sample is taken; third, a value of one is subtracted from each absolute value; finally, the RMS of the data processed in this manner is computed.

For an ideal square wave with a standard deviation of one and a mean of zero, the absolute value of all the samples would be one. Thus, an ideal square wave would have a zero RMS figure-of-merit. This figure-of-merit was calculated for each current/temperature combination in this investigation. For LDA021, measurements were performed at six temperatures and seven drive currents, providing 42 operating conditions (See Figure 4-7). For LDA064, measurements were performed for five temperatures and six drive currents (see Figure 4-8).

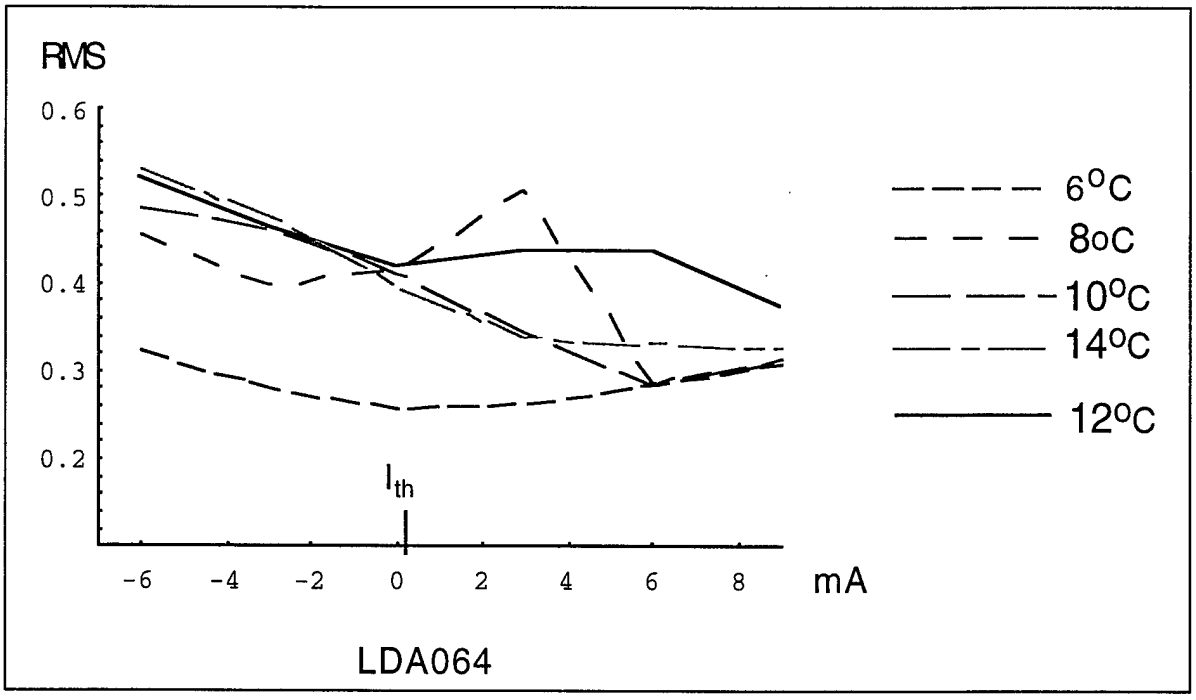

Figure 4-7: RMS deviation from square waves for LDA064.

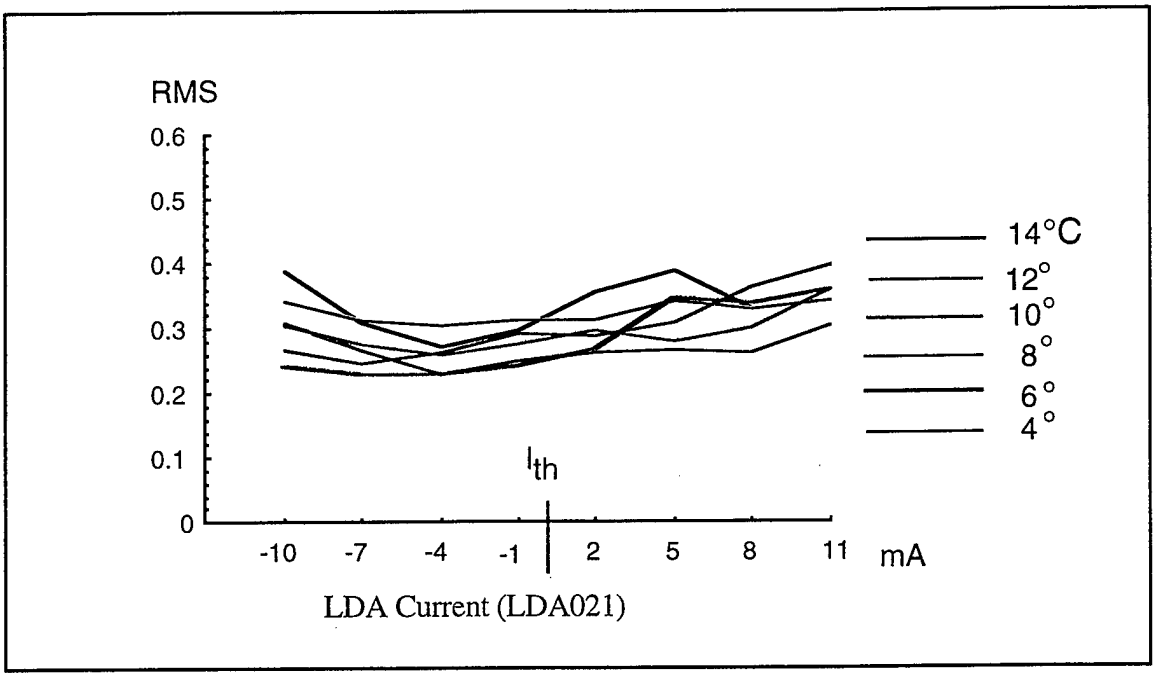

Figure 4-8 RMS deviation from square wave for LDA021.

As shown in Figures 4-7 and 4-8, the measured RMS noise as a function of temperature and current were significantly different for LDA064 and LDA021. LDA064 shows one temperature (8° C) with a very low RMS for all currents. At another temperature (6° C), the RMS for LDA064 exhibits a strong current component. LDA021 does not have two temperatures that similarly vary. LDA021 indicates a minimum noise area below the current threshold for all temperatures.

There is no single criterion for locating the optimum operating region for both LDAs. Different LDAs will react differently to temperature and current variations. Further work is required to determine whether the LDAs can be grouped into classes, with a well defined optimum operating region for each class.

V. Conclusions and Recommendations

A. Conclusions

A theoretical linkage between spectral structure and far field time domain measurements is beyond the scope of this study. However, a qualitative connection might be made between the observed deviation in spectral structure and far field intensity fluctuations. Specifically, both the spectral mode study and the time domain study indicate that there are unit to unit variations. This

investigation does appear to bear out the observation that performance varies as a function of temperature. Furthermore, there appear to be regions of better and worse performance in current-temperature operating space. The results from LDA064 for example, indicate a correlation between the spectral mode and far field (time domain) measurements. Both types of measurements for this unit indicate better performance at higher bias currents, with little dependence on temperature. However, the LDA021 differs and does not support such a correlation.

The effects of varying temperature and current on the LDA behavior indicate that there are regions that produce a lower RMS. This suggests that there probably are regions where a compromised BER can be mitigated simply by finding a new optimum operating regime for a given diode. There is no evidence that a specific I_{min} setting could be calculated apriori, but a global search could determine the optimum settings.

B. Recommendations

1. A theoretical linkage between spectral structure and far field time domain measurements should be explicitly developed. From such a treatment, we can understand how time-dependent excitation of laser and fiber modes can affect intensity distributions in the far field and ultimately, how those excitations affect Bit Error Rate.

2. A subsystem level test should be conducted. That is, the performance of the transmitter component, the LDA, has been characterized. The next step is to determine the effects of the transmitter drive electronics and receiver noise and electronics on the modal response and RMS time-domain response. The subsystem test should measure waveform deviation and RMS for different temperature and current densities as was done in the LDA tests.

3. A complete system level test should then be performed. That is, the BER should be measured as a function of temperature and current.

4. If the subsystem and system level tests bear out the results of the component level tests (i.e., that compensatory changes in current for changes in temperature improve BER) then a step-by-step ground-based implementation plan to identify a new optimum operating point should be developed.

5. We further recommend that for any units anticipated to be implemented in space, that the performance of a given device be "mapped" on the ground, prior to launch. That is, that the modal and RMS response of a transmitter unit be characterized as a function of temperature and drive current, with special

consideration to the region above and below threshold. Although aging on orbit may cause some shift from optimum operating regimes, it is not anticipated that the shift will be significant. Hence, locating a new stable operating point would be a controlled search bounded by the deviation maps.

ACKNOWLEDGMENT

We would like to acknowledge Wendy Lippencott for her invaluable guidance in the modal tests and Michael J. Vilcheck for his dedication and hard work in support of this effort.